

## **THE HEIGHT OF THE SCHOTTKY BARRIER VERSUS THE PHOTOCATALYTIC ACTIVITY OF TiO<sub>2</sub>+Au COMPOSITES UNDER VISIBLE-LIGHT ILLUMINATION**

*Gregor Žerjav, Albin Pintar*

Department of Inorganic Chemistry and Technology, National Institute of Chemistry, Hajdrihova 19,  
SI-1001 Ljubljana, Slovenia  
E-mail: [gregor.zerjav@ki.si](mailto:gregor.zerjav@ki.si)

### **ABSTRACT**

Composites containing different TiO<sub>2</sub> supports (anatase nanoparticles (TNP) and nanorods (TNR)) and 1 wt. % of Au were synthesized using wet impregnation preparation procedure. The size of formed Au ensembles in the composites was influenced by the difference in the zeta potential value (pH<sub>PZC</sub>) of TiO<sub>2</sub> supports. The positive surface charge of TNP nanoparticles during the wet impregnation synthesis positively influenced the formation of Ti<sub>5</sub>-O-Au(III) complex. In turn, the average Au cluster size in the TNP+Au composite was smaller (2.4 nm) than in the TNR+Au composite (9.4 nm), where the surface of the TNR nanorods was negatively charged. The UV-Vis DR spectra of composites exhibited a broad absorption peak at 550 nm, which is typical for the plasmonic behaviour of Au clusters. A detailed XPS analysis of the valence band maxima (VBM) showed that the value of Schottky barrier height (SBH) in the TNP+Au composite (0.31 eV) was almost double compared to the one in the TNR+Au composite (0.16 eV). The visible-light generated “hot electrons” in Au clusters of the TNP+Au composite need more energy and longer time to overcome the SB when injected into the TNP, compared to “hot electrons” generated in the TNR+Au composite exhibiting lower SBH. Due to this obstacle, TNP+Au “hot electrons” have a higher potential to recombine with the generated holes in Au clusters than “hot electrons” injected into the TNR support. The higher specific surface area of the TNR support presents an additional advantage, which prolongs the “lifetime” of electrons in the TNR+Au composite. The electrons can use a larger area to generate reactive oxygen species (ROS) or oxidize adsorbed substrates compared to electrons in the TNP+Au composite.

Key words: TiO<sub>2</sub> nanorods/nanoparticles, Au ensembles, plasmonic noble metal, photocatalysis, Schottky barrier height.

### **INTRODUCTION**

Heterogeneous photocatalysis with a semiconductor oxide as a catalyst has been indicated as highly effective for water remediation [1]. Due to various advantages (high photocatalytic activity, stability in water, low toxicity, moderate price, etc.), titanium dioxide (TiO<sub>2</sub>) has been identified as one of the most suitable catalysts for the heterogeneous photocatalysis aimed for water purification [2]. The drawbacks of TiO<sub>2</sub> are its band-gap energy of 3.0-3.4 eV (charge carriers can be generated only under UV-light illumination) and poor quantum efficiency due to charge carrier recombination [3]. One of the approaches to overcome the drawbacks of TiO<sub>2</sub> is to combine it with noble metal Au [4] and to use the Au plasmonic properties to trigger the catalytic activity of TiO<sub>2</sub> under visible-light illumination. The main mechanisms of plasmonic photocatalysis under visible-light illumination are hot electron generation and injection, plasmonic resonance energy transfer (PRET), and plasmonic heating [5]. At the junction between the Au and TiO<sub>2</sub> a barrier is formed, which is called the Schottky barrier (SB) [6]. Au clusters generate “hot electrons”, if illuminated with light wavelength of which is equal or greater than Au surface plasmon resonance (SPR). The generated “hot electrons” are further injected into the conduction band of TiO<sub>2</sub>. The height of the Schottky barrier (SBH) is influencing the efficiency of the plasmon induced electron injection at the interface between

the Au and TiO<sub>2</sub>. Therefore, an in-depth understanding of the SBH is of crucial importance for the development of plasmonic photocatalysts as the plasmon-driven transfer of “hot electrons” from the noble metal to the semiconductor significantly affects the overall photocatalytic activity of a plasmonic driven photocatalyst [7].

The aim of the present study was to investigate in detail how the textural properties and the zeta potential of anatase TiO<sub>2</sub> supports (nanoparticles (TNP) and nanorods (TNR)) influence the optical, electronic and photocatalytic properties of plasmonic-based TiO<sub>2</sub>+Au composites with 1 wt. % of Au loading. Besides thorough characterization of synthesized solids with several methods (SEM, SEM-EDS, TEM, XRD, N<sub>2</sub> physisorption analyses, UV-Vis DR, recording photoluminescence (PL) spectra of solids, electrochemical impedance spectroscopy (EIS) analysis, etc.), one of the main objectives of the research work was to use XPS technique to determine the height of SB in the prepared TiO<sub>2</sub>+Au photocatalysts and to correlate it with their ability to generate charge carriers under visible-light illumination. Further, we conducted photocatalytic tests in the presence of examined catalysts in a batch slurry reactor under visible-light illumination and using water-dissolved bisphenols (bisphenol A (BPA), bisphenol AF (BPAF), bisphenol S (BPS) and bisphenol F (BPF)) as model organic pollutants.

## RESULTS AND DISCUSSION

The results of SEM and TEM analyses reveal that an average TNP nanoparticle expresses an ellipsoid shape with a 20 nm diameter and a length of 30 nm, whereas on the other hand TNR nanoparticles express a rode-like morphology with a diameter between 8-10 nm and a length of 70-100 nm. The difference in the morphologies of the anatase TiO<sub>2</sub> supports was well expressed also by the results of N<sub>2</sub> physisorption analysis (Table 1).

**Table 1.** Comparison of Au particle size, specific surface area ( $S_{BET}$ ), average pore diameter ( $d_{pore}$ ), total pore volume ( $V_{pore}$ ), anatase TiO<sub>2</sub> crystallite size of studied catalysts, and results of SEM-EDS elemental analysis of TiO<sub>2</sub>+Au composites.

Catalyst	<sup>a</sup> $d_{Au}$ (nm)	$S_{BET}$ (m <sup>2</sup> /g)	$d_{pore}$ (nm)	$V_{pore}$ (cm <sup>3</sup> /g)	Anatase crystallite size (nm)	Content (wt. %)		
						Ti	O	Au
TNR	/	105	19.3	0.57	16.7		/	
TNR+Au	9.4	93	18.9	0.44	16.5	57.4	41.9	0.7
TNP	/	82	14.8	0.30	20.9		/	
TNP+Au	2.4	68	16.1	0.27	20.2	63.3	35.8	0.9

<sup>a</sup>Au particle size was determined by counting more than 100 particles from acquired TEM images.

Further, the TEM analysis shows that the morphology of TNP and TNR supports did not change during the deposition of Au and that the morphology of TiO<sub>2</sub>+Au composites is dominated by the TiO<sub>2</sub> support. The presence of Au in the composites was confirmed by the results of SEM-EDS analysis (Table 1). The XRD patterns of prepared materials illustrated diffraction peaks indicative for anatase TiO<sub>2</sub> and imply that the TiO<sub>2</sub> supports were stable during the Au deposition procedure and calcination. Also, the values of anatase crystallite size calculated from the corresponding width of the (001) diffraction peak ( $2\theta=25^\circ$ ) by means of the Scherrer formula (Table 1), show that the anatase crystallite size of the composites was not affected by the catalyst preparation procedure. Average size of Au ensembles in the composites calculated from the TEM analysis (Table 1) show that the size of Au ensembles depends on the employed TiO<sub>2</sub> support as the average size of Au clusters in TNP+Au sample was 2.4 nm and 9.4 nm in the TNR+Au solid. The  $pH_{PZC}$  values of bare TiO<sub>2</sub> supports were significantly different with the  $pH_{PZC}$  value of 2.8 for the TNR sample and 7.2 for the TNP material. The pH

value of the Au precursor solution ( $\text{HAuCl}_4 \times 3\text{H}_2\text{O}$ ) during the composite preparation procedure was 3.4, which means that the surface of TNP nanoparticles was protonated and the surface of TNR nanorods deprotonated. The positive charge of the TNP surface beneficially influences adsorption of the  $[\text{Au}(\text{OH})_3\text{Cl}]^-$  complex through a strong electrostatic attraction, compared to the negative charge of the TNR surface. UV-Vis DR spectra of bare  $\text{TiO}_2$  supports show the typical behaviour of anatase  $\text{TiO}_2$  with a strong absorption in the UV range (200-350 nm) of the light spectra and consequently a large band gap of 3.26 eV. The spectra of the  $\text{TiO}_2+\text{Au}$  composites display additional spectral response in the visible-light range between 500 and 600 nm attributed to the plasmonic behaviour of the Au ensembles. The difference in the size of Au clusters in the composites (Table 1) might be the reason that the TNR+Au composites expressed higher intensity in the visible-light absorbance. The recombination of photo-induced electrons and holes releases energy in the form of PL emissions, therefore the intensity of the PL signal is proportional to the electron-hole recombination rate. The decrease in the PL intensities observed in the PL spectra belonging to  $\text{TiO}_2+\text{Au}$  composites is attributed to the formation of a Schottky barrier at the  $\text{TiO}_2$  support/Au ensemble junction, which can act as an electron sink thus suppressing the electron-hole recombination. Regarding the  $\text{TiO}_2+\text{Au}$  composites, the PL intensity of TNR+Au composite was lower than the one of TNP+Au sample, so the recombination rate of charge carriers in the TNR+Au composite is lower. The ability of prepared photocatalysts for the separation of photo-generated electron-hole pairs upon illumination with visible light was tested by the EIS measurements. The EIS results show that  $\text{TiO}_2+\text{Au}$  composites are able to generate significantly more visible-light generated charge carriers than bare  $\text{TiO}_2$  supports, which could be due to the plasmon properties of the Au ensembles. Further, EIS measurements reveal that the TNP+Au composite is able to generate less charge carriers than the TNR+Au composite. The results of VBM measurements of the investigated materials are illustrated in Fig. 1. The VBM positions of the measured materials with respect to Fermi level ( $E_F$ ) were found to be 3.07 eV for TNP, 3.09 eV for TNR, 2.76 eV for TNP+Au and 2.92 eV for TNR+Au samples, respectively. The VBM of the composites shifts toward lower binding energies as a consequence of the charge transfer and formation of a Schottky barrier height (SBH) at the junction between  $\text{TiO}_2$  support and Au clusters. The SBH values for the TNP+Au and TNR+Au composites were found to be equal to 0.31 and 0.16 eV, respectively.

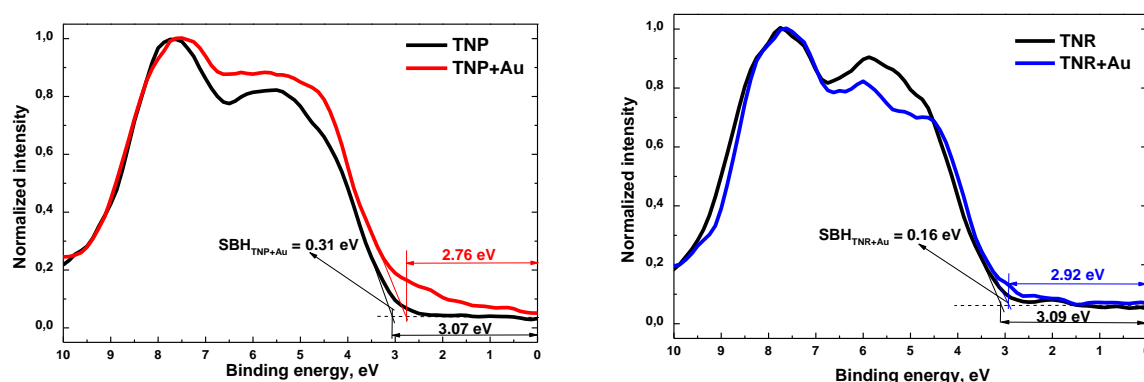


Figure 1. Determination of VBM of pure  $\text{TiO}_2$  supports and  $\text{TiO}_2+\text{Au}$  composites by means of XPS analysis.

The prepared catalysts were investigated in a batch slurry reactor toward degradation of water-dissolved bisphenols under visible-light illumination. In the given range of operating and reaction conditions, pure  $\text{TiO}_2$  supports show almost no or only minor ability to degrade bisphenols. However, significant decrease of concentration of model organic pollutants was obtained in the presence of  $\text{TiO}_2+\text{Au}$  composites. The results show that regardless which

bisphenol analogue is used, the TNR+Au composite was able to degrade/mineralize higher amounts of bisphenols in comparison to the TNP+Au composite. This fact can be ascribed to the difference in the SBH (Fig. 1) and higher  $S_{\text{BET}}$  of the TNR+Au composite (Table 1), which makes the latter more accessible to water-dissolved molecules of organic pollutants in comparison to the TNP+Au sample. With the use of TNR+Au composite 75 % of BPA and 96 % of BPF were degraded; on the other hand, with the same composite 21 % of BPAF and 17 % of BPS were degraded after 120 min of visible-light illumination. The same trend was observed when we measured the mineralization extent ( $\text{TOC}_M$ ) at the end of photocatalytic oxidation runs. Based on the measured conversions as well as extent of mineralization, the examined bisphenols can be divided into two groups: BPA and BPF on one side, and BPAF and BPS on the other. The measured differences in degradation rates of the bisphenols can be ascribed to differences in their chemical structures with the consequence that different pathways of their degradation occur. This results in different degradation products which express different resistances toward reactions with visible-light generated charge carriers and ROS.

## CONCLUSION

Wet impregnation technique was used to produce  $\text{TiO}_2$ +Au composites with different  $\text{TiO}_2$  supports (anatase nanoparticles (TNP) and nanorods (TNR)) and 1 wt. % Au loading. The results of SEM and TEM analyses show that the morphology of TNP and TNR supports did not change during the preparation procedure and that the  $\text{TiO}_2$ +Au morphologies are dominated by the morphology of  $\text{TiO}_2$  supports. The average size of Au ensembles in the TNP+Au and TNR+Au composites was 2.4 and 9.4 nm, respectively. The Au ensembles in  $\text{TiO}_2$ +Au composites exhibited plasmonic behaviour as a broad absorption peak in the region between 500 and 600 nm was measured in the UV-Vis DR spectra. The TNR+Au composite exhibited a higher amount of visible-light generated charge carriers (EIS measurements) and lower recombination of charge carriers (PL measurements) rate than the TNP+Au composite. Detailed XPS analysis of VBM suggests that this is attributed to differences in the SB heights of the  $\text{TiO}_2$ +Au composites. The visible-light generated electrons in Au ensembles of the TNR+Au composite need lower energy to overcome the SBH of 0.16 eV, when they are injected into the valence band of TNR, compared to electrons in the TNP+Au composite, where the SBH is 0.31 eV. Another property that beneficially influences the photocatalytic activity of TNR+Au composite is its larger specific surface area. Experiments of photocatalytic oxidation of water-dissolved bisphenols over  $\text{TiO}_2$ +Au composites showed that visible-light generated charge carriers and ROS were successfully used for their oxidation and mineralization.

## REFERENCES

- [1] Y. Deng, R. Zhao, *Curr. Pollution Rep.*, 2015, **1**, 167-176.
- [2] M.R. Hofmann, S.T. Martin, W. Choi, D.W. Bahnemann, *Chem. Rev.*, 2002, **95**, 69-96.
- [3] Y. Cong, J.L. Zhang, F. Chen, M. Anpo, *J. Phys. Chem. C*, 2007, **111**, 6976-6982.
- [4] D. Wang, S.C. Pillai, S.-H. Ho, J. Zeng, Y. Li, D.D. Dionysiou, *Appl. Catal. B*, 2018, **237**, 721-741.
- [5] X. Chen, H.Y. Zhu, J.C. Zhao, Z.F. Zheng, X.P. Gao, *Angew. Chemie Int. Ed.*, 2008, **47**, 5353-5356.
- [6] X. Chen, S. Shen, L. Guo, S.S. Mao, *Chem. Rev.*, 2010, **110**, 6503-6570.
- [7] M.S. Arshad, Š. Trafela, K. Žužek Rožman, J. Kovač, P. Djinović, A. Pintar, *J. Mater. Chem. C*, 2017, **5**, 10509-10516.